Electrospun Doping of Carbon Nanotubes and Platinum Nanoparticles into the β-Phase Polyvinylidene Difluoride Nanofibrous Membrane for Biosensor and Catalysis Applications

Panpan Zhang,[†] Xinne Zhao,[†] Xuan Zhang,[†] Yue Lai,[†] Xinting Wang,[†] Jingfeng Li,[‡] Gang Wei,*[,‡] and Zhiqiang Su*[,†]

[†]Beijing Key Laboratory on Preparation and Processing of Novel Polymeric Materials, Beijing University of Chemical Technology, 100029 Beijing, China

[‡]Hybrid Materials Interfaces Group, Faculty of Production Engineering, University of Bremen, D-28359 Bremen, Germany

ABSTRACT: A novel β-phase polyvinylidene difluoride (PVDF) nanofibrous membrane decorated with multiwalled carbon nanotubes (MWCNTs) and platinum nanoparticles (PtNPs) was fabricated by an improved electrospinning technique. The morphology of the fabricated PVDF−MWCNT−PtNP nanofibrous membrane was observed by scanning electron microscopy, and the formation of high β-phase in the hybrid nanofibrous membrane was investigated by Fourier transform infrared spectroscopy and differential scanning calorimetry. The uniform dispersion of MWCNTs and PtNPs in the PVDF hybrid nanofibrous membrane and their interaction were explored by transmission electron microscopy and X-ray diffraction. For the first time, we utilized this created PVDF−MWCNT−PtNP nanofibrous membrane for biosensor and catalysis applications. The nonenzymatic amperometric biosensor with highly stable and sensitive, and selective detection of both H_2O_2 and glucose was successfully fabricated based on the electrospun PVDF−MWCNT−PtNP nanofibrous membrane. In addition, the catalysis of the hybrid nanofibrous membrane for oxygen reduction reaction was tested, and a good catalysis performance was found. We anticipate that the strategies utilized in this work will not only guide the further design of functional nanofiber-based biomaterials and biodevices but also extend the potential applications in energy storage, cytology, and tissue engineering.

KEYWORDS: nanofibrous membrane, electrospun, biosensor, catalysis, application
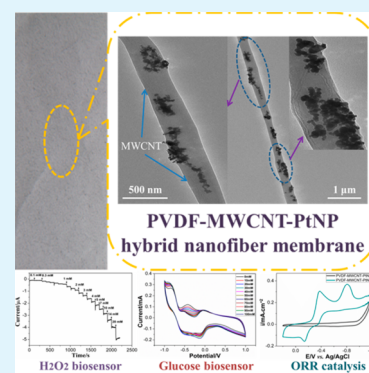
INTRODUCTION

In recent years, electrochemical biosensors have attracted much attention due to their importance in both basic and applied studies.[1] With the development of biotechnology and nanotechnology, the functional biological sensor devices, including enzyme sensor,[2] microbial sensor,[3] immunosensor,[4] tissue sensor,[5] and DNA sensor,[6] have shown huge growth potential and space. Among them, the analytical determination of hydrogen peroxide (H_2O_2) and glucose raised extensive attention, which are mainly ascribed to their extended applications in diabetes mellitus, pharmacy, clinical analysis, and food examination.[7−10] Compared to the conventional biosensors, many novel biosensors have been fabricated based on the novel design concepts and emphasis. For instance, many techniques, such as enzyme modification,[11,12] fluorescence labeling,[13] magnetism,[14] molecular imprinting,[15] and electrochemistry,[16] have been employed to detect glucose previously. It is well-known that electrochemical detection (enzymatic and nonenzymatic) of H_2O_2 and glucose is facile, stable, and effective.[1,16,17] In addition, the enzymatic sensor has some obvious disadvantages like low sensitivity, unstable immobilization, long response time, and short service life.[2,18] Therefore, the nonenzymatic electrochemical sensor has attracted more interest due to its simplicity, high stability, and good reproducibility.[19,20]

During the fabrication and application of nonenzymatic electrochemical sensors, the selection of a suitable catalyst for detection plays an important role. Metal nanoparticles (MNPs) are the major promising candidates for the fabrication of electrochemical sensors. It has been reported that Au, Ag, Pt, Pd, Cu, and Ni nanoparticles and their derivatives possess very good electrochemical activity toward H_2O_2 and glucose, and these MNPs have been widely used as biosensor materials.[21−26] PtNPs occupy the most important and irreplaceable position due to their excellent electrochemical performances. In addition, PtNPs are of interest because of their high stability and activity for oxygen reduction reaction (ORR). Some of the most successful ORR catalysts to date (such as the Pt/Au cathodes) have contained Pt-based metals.[27,28] Meanwhile, carbon nanotubes (CNTs) have been also widely used as ideal catalyst supporting materials due to their unique electrical, mechanical, and structural, and chemical properties.[29−31] Therefore,

combinations of CNTs with PtNPs have been carried out to synthesize CNT−PtNP hybrids with enhanced electrochemical performances.[32−36] For example, Luong et al. fabricated an electrochemical glucose biosensor based on combining PtNPs with single-walled carbon nanotubes (SWCNTs),[32] and this biosensor revealed higher sensitivity than that fabricated with pure PtNPs and CNTs. Shen and co-workers constructed a Pt−CNT biosensor with the incorporation of glucose oxidase within the Pt−CNT−silicate matrix[33] and found that the fabricated biosensor responded more sensitively to glucose than CNT- and PtNP-based biosensors.

Electrospinning is a useful technique that can be utilized to create CNT−MNP nanofibrous hybrids. Electrospinning has been used as an efficient technique for the fabrication of polymer or polymer matrix multifunctional hybrid nanofibers with length-controlled, oriented, uniform diameter and high surface to mass ratios.[37] However, until now only very few studies focused on the nonenzymatic electrochemical biosensors and biocatalysts fabricated by electrospinning the polymer−CNT−MNP nanofibrous membrane on electrodes.[38−40] Previously, we created the polyurethane nanofibers filled with CNTs and AgNPs by electrospinning and applied the created hybrid nanofibers for the H_2O_2 biosensor.[41]

Polyvinylidene difluoride (PVDF) and its copolymers have been utilized as sensors, actuators, energy generators, and switches because of its piezo-, pyro-, and ferroelectric properties.[42−44] As a typical example of an organic piezoelectric semicrystalline polymer, PVDF with β crystal structure has good piezoelectric property uniquely. To obtain high β-phase PVDF, some techniques like high-pressure crystallization, uniaxial hot stretching, and high voltage polarization have been employed.[45,46] Recent developments on the fabrication of ferroelectric fibers using electrospinning have opened up new exciting opportunities for the preparation of fiber-based nanodevices.[47,48] For example, Andrew et al. demonstrated the effects of the electrospinning processing on the formation of the α- and β-phase PVDF.[48] It can be clearly demonstrated that electrospinning is simple, efficient, and eco-friendly compared with other techniques. We expected that the fabrication of β-phase PVDF membrane doped with MWCNTs and PtNPs will benefit the creation of functional hybrid nanofiber-based devices with piezo-, pyro-, and ferroelectric properties and further promote their potential applications in biosensors and electrocatalysis.

Herein, we first utilized an improved electrospinning technique to directly fabricate a novel piezoelectric β-phase PVDF hybrid nanofibrous membrane decorated with MWCNTs and PtNPs (PVDF−MWCNT−PtNP) on glass carbon electrodes (GCEs), which can serve as the functional materials for H_2O_2 and glucose nonenzymatic biosensors and oxygen reduction reaction (ORR) catalysis. Our technique for preparing functional devices is environmentally friendly, time saving, highly efficient, and highly reproducible. With the help of electrospinning, MWCNTs can be well dispersed and aligned in the created PVDF nanofibers, which can facilitate both the electron transfer and the uniform dispersion of PtNPs along nanofibers. In addition, the electrospun nanofibrous membranes are three-dimensional structures with high surface area ratio to volume, which is beneficial to the adsorption of electrolytes and the diffusion of reactants. The special structure features result in highly stable, sensitive, and selective detection of H_2O_2 and glucose. Moreover, a good catalysis performance for ORR was demonstrated. Our results not only demonstrate the powerful ability of electrospinning for creating β-phase PVDF nanofibers but also confirm the good performances of the electrospun PVDF−MWCNT−PtNP nanofibrous membrane as biosensors and catalyst.

■ EXPERIMENTAL SECTION

Materials. MWCNTs (>90% purity, OD 10−15 nm, ID 2−6 nm, length 0.1−10 μm), PtNPs (<50 nm particle size), and D-(+)-glucose (≥99.5% purity) were purchased from Sigma-Aldrich. Ascorbic acid (AA), uric acid (UA), and dopamine (DA) were obtained from J&K Scientific Ltd. (Beijing, China). PVDF (MW = 600 000, product model FR904) powder was supplied by Shanghai 3F New Material Co., Ltd. (Shanghai, China) and used as-received. *N*-Dimethylformamide (DMF), H_2O_2 (analytical grade, 30% aqueous solution), acetone, potassium hydroxide (KOH), disodium hydrogen phosphate (Na_2HPO_4), and sodium dihydrogen phosphate (NaH_2PO_4) were purchased from Beijing Chemicals Co., Ltd. (Beijing, China). All chemicals used in this work were analytical reagents and obtained from commercial sources and directly used without additional purification. The water used was purified through a Millipore system (~18.2 MΩ·cm).

Electrospinning PVDF, PVDF−PtNP, PVDF−MWCNT, and PVDF−MWCNT−PtNP Nanofibers. To prepare spinning solutions with different components, the solvent has been made using a mixture of DMF and acetone (3:2, v/v). PtNPs and MWCNTs were first dispersed in the mixture solvent with an ultrasonic cleaner operating at 40 kHz for 1.5 h. Then the weighed PVDF was added and dissolved in the dispersions. Finally, the resulting dispersions were homogeneous and stable after ultrasonication for 1.5 h. Four types of spinning solutions (PVDF, PVDF−PtNP, PVDF−MWCNT, and PVDF−MWCNT−PtNP) were prepared successfully. The concentrations of PVDF, MWCNTs, and PtNPs were 11, 1, and 0.1 wt % in all the solutions, respectively. These dispersions were loaded into plastic 10 mL plastic syringes with a 16 gauge blunt tip needle and were dispensed at a rate of 0.3−0.5 mL·h^{-1} during electrospinning. All the samples were electrospun with an applied voltage of 12 kV at a distance of 12 cm from the needle tip to the collector surface of tinfoil.

Preparation of Nanofibrous Membrane Modified GCE. The homemade electrospinning setup utilized in this work is schematically shown in Figure 1. We added a pair of parallel auxiliary electrodes
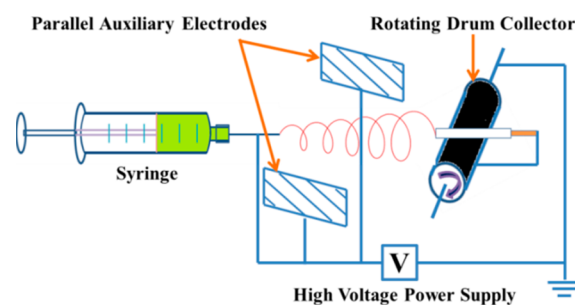

Figure 1. Schematic of the electrospinning apparatus for preparing nanofibrous membrane modified GCE.

between the spinneret and drum collector. The two symmetric, rectangular, and auxiliary aluminum electrodes were operated at a high voltage of the same polarity as the needle but with an adjustable potential controlled by another independent high voltage power supply. The parallel placed auxiliary electrodes can generate a symmetrical auxiliary electric field that can damp the bending instability of the electrospinning jet perpendicular to the direction of alignment, to enable aligned deposition. GCE was fixed on the drum collector, and both the drum collector and GCE were connected to the ground. To make sure to spin fibers onto the surface of GCE, we made a promotion on the standard electrospinning setup by adding a pair of parallel auxiliary electrodes. It takes 2 min to deposit the nanofibers onto the surface of the GCE for each sample. The GCE was polished
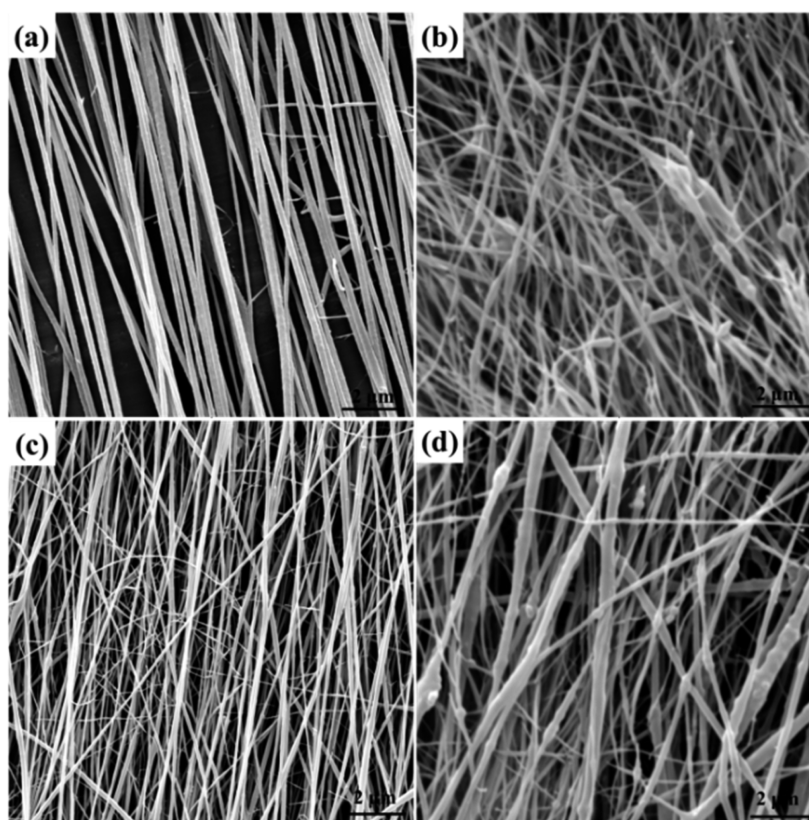
Figure 2. SEM images of electrospun PVDF hybrid membranes with different nanofillers (MWCNTs or PtNPs): (a) pure PVDF, (b) PVDF–PtNP, (c) PVDF–MWCNT, and (d) PVDF–MWCNT–PtNP.
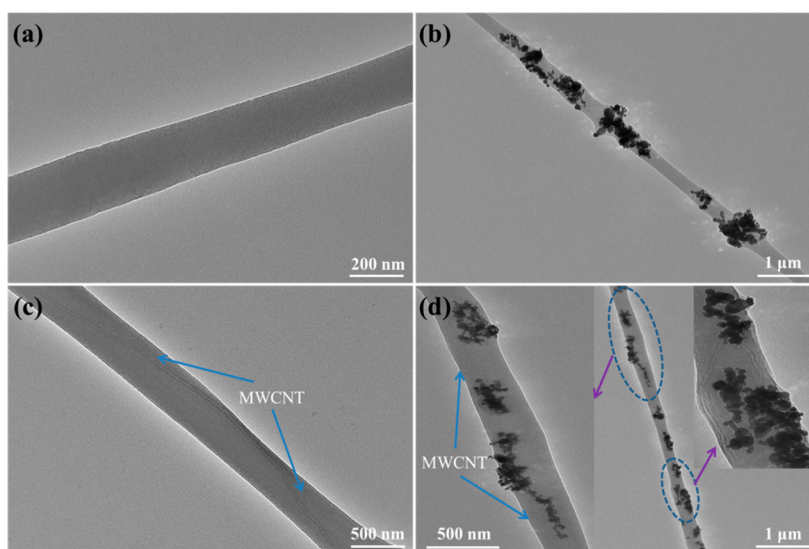

Figure 3. TEM photographs of (a) PVDF, (b) PVDF–PtNP, (c) PVDF–MWCNT, and (d) PVDF–MWCNT–PtNP hybrid nanofibers.

with 1 and 0.3 μm alumina slurry before electrospinning and then successively washed with ethanol and distilled water in an ultrasonic bath. Finally, the fabricated nanofibrous membrane modified GCEs were dried in air for biosensor application.

Characterization Techniques. SEM experiments were performed on a JSM-6700F scanning electron microscope (JEOL). The sample surface was coated with a thin Au layer to protect the surface layers from ion beam damage. TEM images were taken by a Tecnai G²20 transmission electron microscope (FEI) with an accelerating voltage of 200 kV, and samples were prepared by directly electrospinning onto the copper grid. Differential scanning calorimetry (DSC, PerkinElmer-

Diamond), Fourier transform infrared spectroscopy (FTIR, Nicolet 6700, Thermo-Fisher, USA), and X-ray diffraction (XRD, Rigaku D/max-2500 VB+/PC) were used to compare the morphologies and structures of PVDF, PVDF–PtNP, PVDF–MWCNT, and PVDF–MWCNT–PtNP hybrid nanofibrous membranes.

Electrochemical Experiments and Biosensor Platform. All the electrochemical experiments were carried out using an electrochemical workstation (CHI760D, Chenhua, Shanghai) at room temperature. A conventional three-electrode system was employed with a modified GCE as a working electrode, a Pt wire as an auxiliary electrode, and a KCl saturated calomel electrode (SCE) or Ag/AgCl electrode as a
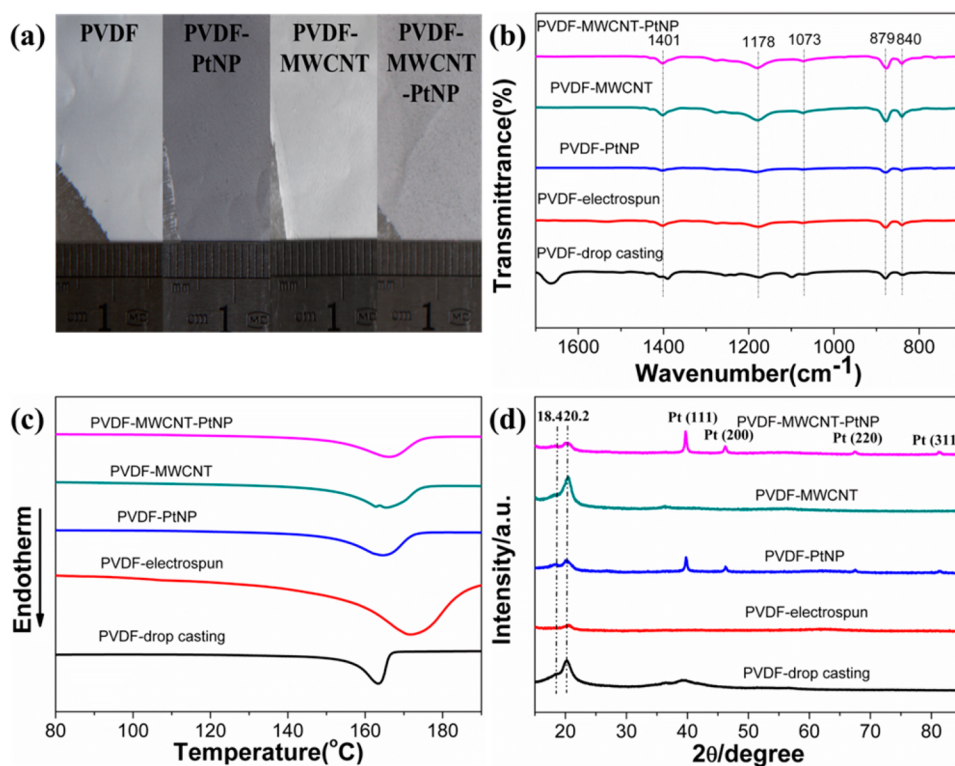
Figure 4. Crystalline phase characterizations of electrospun PVDF-based hybrid nanofibers: (a) optical photographs, (b) FTIR spectra, (c) DSC thermograms, and (d) XRD patterns.

reference electrode. The test solution in biosensor application was phosphate buffer solution (PBS, 0.1 M) with pH = 7.6, which was prepared with 0.1 M NaH_2PO_4 and 0.1 M Na_2HPO_4 and deoxygenated with highly pure nitrogen for 20 min before electrochemical experiments. The test solution in electrocatalysis application was KOH solution (0.1 M) under deoxygenating with highly pure N_2 or rich-oxygenating with highly pure O_2 for 1 h. The curves of cyclic voltammograms (CVs) in this work were collected after six scan numbers under steady-state conditions. Amperometric measurements were carried out under stirred conditions.

RESULTS AND DISCUSSION

Morphology Characterization of Electrospun Nanofibrous Membranes on GCEs. The morphologies of the electrospun PVDF, PVDF−PtNP, PVDF−MWCNT, and PVDF−MWCNT−PtNP nanofibrous membranes on GCEs were observed by SEM first. It can be clearly seen that all the fabricated nanofibrous membranes are three-dimensional porous structures. In addition, the electrospun nanofibers of both PVDF and PVDF−MWCNT are uniaxial-oriented, and the surface of the nanofibers is smooth, as seen in Figure 2a and c. The width of the nanofibers is about 150−300 nm. In contrast, the surface of the PVDF−PtNP hybrid nanofibers is rough, on which there are many obvious nodules (Figure 2b). We suggest that these nodules are ascribed to the aggregation and heterogeneous distribution of PtNPs in PVDF nanofibrous substrate. It is surprising that the electrospun PVDF−MWCNT−PtNP hybrid nanofiber is less rough and with less distinct nodules compared to the PVDF−PtNP nanofiber (Figure 2d). It can be concluded that the MWCNTs have nonspecific interaction with PtNPs, which result in the favorable distribution of PtNPs in the PVDF matrix.

The dispersion of PtNPs and MWCNTs in PVDF nanofibers was further investigated with TEM, and the corresponding result is shown in Figure 3. Pure PVDF nanofiber without further hybridization is smooth (Figure 3a). After introduction of PtNPs into the PVDF nanofibers, it is clear that the PtNPs disperse throughout the PVDF matrix discretely (Figure 3b). The TEM image of electrospun PVDF−MWCNT nanofibers indicates that the MWCNTs are aligned and oriented along the axis of PVDF nanofibers (Figure 3c). Due to the high elongation of the polymer jet during the electrospinning process, the CNTs tend to orient along the fiber axis and are embedded in the fiber core.[49,50] Therefore, electrospinning is an efficient processing method to produce CNT−polymer nanofibers with the CNTs orienting to the axes of the as-spun nanofibers. There is a fast growing interest in applying this technique to produce nanofibers using various polymers. In addition, it is interesting that the PtNPs tend to attach onto the side walls of MWCNTs, and at the same time MWCNTs serve as bridges to connect the dispersive PtNPs together in PVDF−MWCNT−PtNP hybrid nanofibers (Figure 3d and its insets). The assembly of MWCNTs and PtNPs can effectively facilitate the electron transfer, thus boosting the conductivity and improving the electrocatalytic performance of the fabricated materials.

Crystalline Phase Determination of PVDF. The optical photographs of the four electrospun PVDF-based membranes on aluminum foil are displayed in Figure 4a. We can see all membranes are continuous, uniform, and porous. However, the difference in appearance between different membranes can be identified distinctly, in which the block points and gray appearance result from the additives of MWCNTs and PtNPs. It is known that PVDF has five different crystalline phases: α, β, γ, δ, and ε.[51] Among these crystalline phases, the most common one is the α-phase, while only the polar β-phase can perform strong piezoelectric polarization for functional devices.

Table 1. Effects of the Electrospinning Process on the Crystallinity and the Contents of α- and β-Phase of PVDF

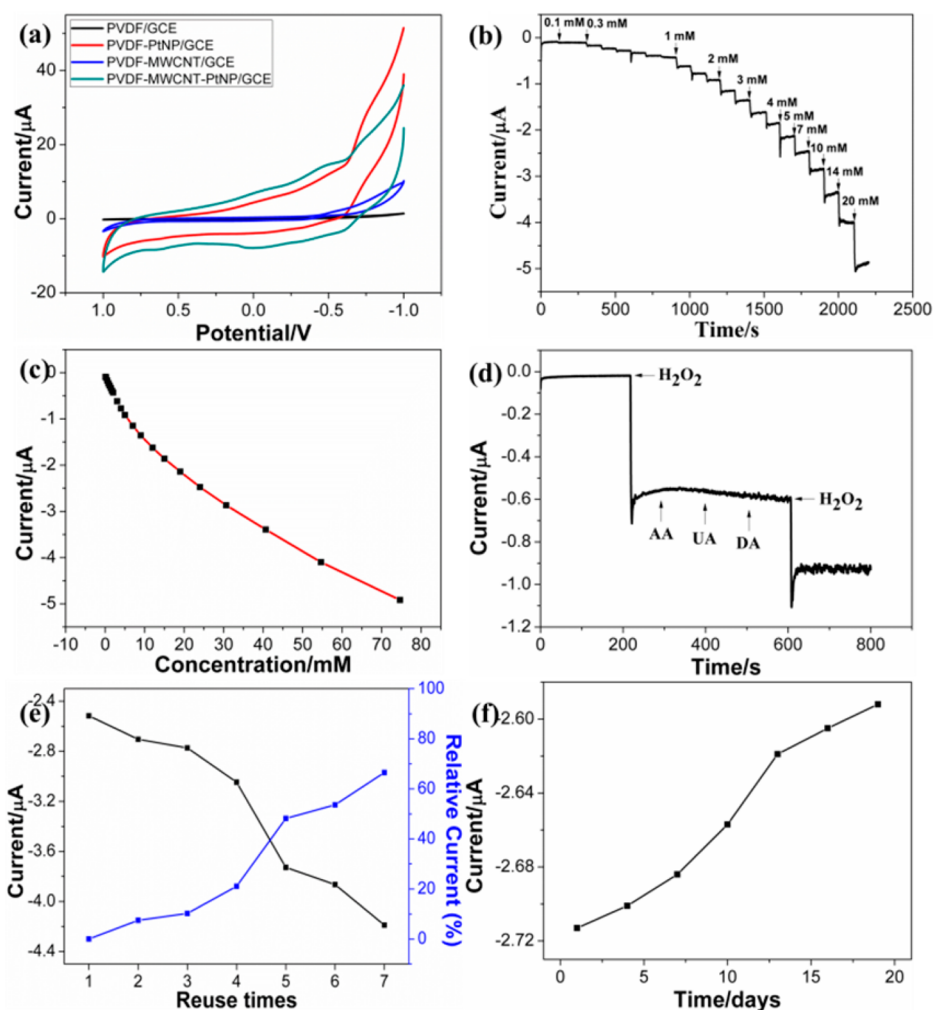| samples	crystallinity/%	content of α phase/%	content of β phase/%
PVDF−drop casting	62.32	82.4	17.6
PVDF−electrospun	77.16	18.1	81.9
PVDF−PtNP	70.51	25.7	74.3
PVDF−MWCNT	73.37	22.6	77.4
PVDF−MWCNT−PtNP	72.79	23.2	76.8

Figure 5. Electrochemical H_2O_2 biosensing: (a) CVs of GCEs modified with PVDF, PVDF−PtNP, PVDF−MWCNT, and PVDF−MWCNT−PtNP hybrid nanofibrous membranes. (b) $I−T$ response of PVDF−MWCNT−PtNP hybrid nanofibrous membrane modified GCE in 0.1 M PBS with successive addition of H_2O_2 at 0.6 V vs SCE. (c) Calibrated line. (d) Selectivity of biosensor. (e) Reusability and (f) long-term storage stability in response to 5 mM H_2O_2.

The formation of high piezoelectric β-phase in hybrid nanofibers was determined with FTIR, DSC, and XRD, respectively. Figure 4b presents the FTIR spectra of PVDF-based hybrid membranes by doping different components. Usually, the peaks appearing at 765, 1178, and 1393 cm^{-1} are attributed to the α-phase, while the peaks at 840, 879, 1073, and 1401 cm^{-1} are indexed to the β-phase.[52,53] It should be noted that the characteristic -phase absorption bands that are commonly seen for bulk PVDF are not evident in the spectra recorded for the electrospun nanofibers. To investigate the crystallization behavior of PVDF upon the electrospinning and incorporation of MWCNTs and PtNPs, the first heating DSC traces of PVDF hybrid nanofibers and PVDF drop casting film were carried out. As shown in Figure 4c, the melting

temperature (T_m) obtained from the endothermic peak is 163 °C for pure PVDF drop casting film, and the T_m of all electrospun samples shows an obvious shift toward higher temperature compared to the cast sample, which indicates that the high extension of the electrospun jet can induce the crystallization of PVDF and cause an increase in the crystallinity, like the strain-induced crystallization. Also, the addition of MWCNTs and PtNPs into the PVDF nanofibers leads to a slight shift toward lower T_m, as well as a decrease of crystallinity. We suggest that the addition of MWCNTs and PtNPs prevents the polymer from forming perfect crystals and results in the depression of T_m.[54]

Figure 4d shows the XRD patterns of the obtained nanofibrous membranes. The peaks reveal characteristic
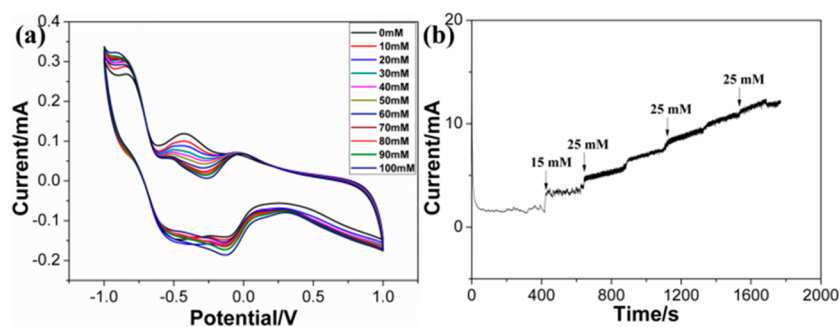
Figure 6. Electrochemical glucose biosensing: (a) CVs of GCEs modified with the PVDF−MWCNT−PtNP hybrid nanofibrous membrane under different glucose additions. (b) $I−T$ response of the PVDF−MWCNT−PtNP hybrid nanofiber modified GCE in 0.1 M PBS with successive addition of glucose at −0.413 V vs SCE.

reflections of both the α- and β-phase at 18.4°, 20.2°, 36.1°, 39.8°, and 56.3° for the PVDF substrate prepared by drop casting.[47] However, it is obvious that the peak at 20.2° (β-phase) for the four electrospun membranes is of strongest intensity compared to that of other peaks, and the peak at 18.4° (α-phase) becomes weaker. We suggest that the electrospun samples have the β-phase as the dominant crystal phase. Furthermore, the other related peaks are not seen obviously, which may suggest that a crystalline transition from the α- to β-phase occurs by electrospinning. In addition, the four strong diffraction peaks for PVDF−PtNP and PVDF−MWCNT−PtNP hybrid nanofibrous membranes are observed at 39.7°, 46.2°, 67.5°, and 81.3°, which could be associated with the (111), (200), (220), and (311) planes of the embedded PtNPs, respectively (JCPDS no. 87-0640). Furthermore, we calculated the crystallinity and α- and β-phase contents of the drop casting and four electrospun samples. As shown in Table 1, the contents are consistent with the upward analysis. With the high voltage and high-speed rotating drum collector, the stretch and polarization effects are imposed on the nanofibers. Separately, the intensive stretch can transform the crystal morphology from the α- to β-phase, and the polarization progress can rearrange the dipole moment along the electric field. On the basis of the above results of FTIR, DSC, and XRD, we prove that the electrospinning process leads to the variation of crystalline structure of PVDF and enhances the β-phase of created PVDF nanofibers.

Biosensor Applications. In a previous report, Halaoui and co-workers investigated the assembly of 2.5 nm random arrayed polyacrylate-capped PtNPs assembling in poly-(diallydimethylammonium chloride) and further explored its potential application for amperometric detection of H_2O_2.[23] We expected that the combination of PtNPs with MWCNTs will improve the conductivity and catalysis performance of the electrospun hybrid nanofibrous membrane. In our study, all the nanofiber-modified GCEs were fabricated by directly electro-spinning the PVDF−MWCNT−PtNP nanofibers onto the polished GCEs in 2 min. Then we investigated the as-spun hybrid nanofibrous membrane as a novel material for fabricating electrochemical H_2O_2 and glucose biosensors, as well as ORR catalyst.

Figure 5a displays the typical CVs of PVDF, PVDF−PtNP, PVDF−MWCNT, and PVDF−MWCNT−PtNP nanofibrous membrane modified GCEs in the presence of 5 mM H_2O_2. It is clear that both PVDF and PVDF−MWCNT membrane modified GCEs show no redox processes, and the PVDF−PtNP modified GCE presents a small current response and a

broad reduction peak. Meanwhile, the PVDF−MWCNT−PtNP nanofibrous membrane modified GCE demonstrates a reduction peak at about 0.6 V with an obvious positive shift for both the onset potential and current peak. Therefore, we selected 0.6 V as the applied potential for $I−T$ measurement. Figure 5b shows a stable response over the long period test and rapid increase in the cathodic current as a result of the reduction of H_2O_2 upon adding H_2O_2 solutions with different concentrations. The calibration curve (Figure 5c) indicates a regular response to H_2O_2, and the range of the H_2O_2 detection is from 0.1 to 75 mM. Compared to previous reports toward the H_2O_2 sensor, our H_2O_2 biosensor has a similar low detection limit of about 0.61 μM.[9,11]

The selectivity test of this H_2O_2 biosensor is shown in Figure 5d, which compares the amperometric response for three relevant electroactive species, such as ascorbic acid (AA), uric acid (UA), and dopamine (DA). No interference and response was observed at the potential of 0.6 V, indicating the high selectivity toward the detection of H_2O_2. The reuse stability of the PVDF−MWCNT−PtNP hybrid nanofibrous membrane modified GCE was also assessed in Figure 5e, showing that the repeated usage of the created biosensor is possible, at least 6 times. Significant reduction in current after 7 times of use is depicted, which may be ascribed to the detachment of the membrane from the electrode. Furthermore, the long-term stability of the PVDF−MWCNT−PtNP hybrid nanofibrous membrane modified GCE was explored over a 15-day period (Figure 5f). The fabricated sensor was stored in the refrigerator at 4 °C and measured every 2−4 days. The result shows that the catalytic current response maintains more than 95.5% of its initial value in response to 5 mM H_2O_2 after 15 days, indicating an acceptable stability of our H_2O_2 biosensor.

The potential application of the PVDF−MWCNT−PtNP nanofibrous membrane modified GCE for glucose sensing was also carried out. Although the glucose sensor has been studied for many years, the high sensitivity, high stability, and low limit of detection are still the eternal goals for the design.[55] Electrospinning is a completely new and facile technique for fabricating the nonenzymatic glucose biosensor.

Figure 6a shows the CVs of the PVDF−MWCNT−PtNP hybrid nanofibrous membrane modified GCE upon adding glucose solutions with different concentrations. It is clear that the two peak potentials located at −0.41 and −0.19 V keep stable with the change of the concentrations of analytes. The intensity of the oxidation peak (−0.19 V) increased, while the intensity of the reduction peak (−0.41 V) decreased with the raising of glucose concentrations. We suggest that this change
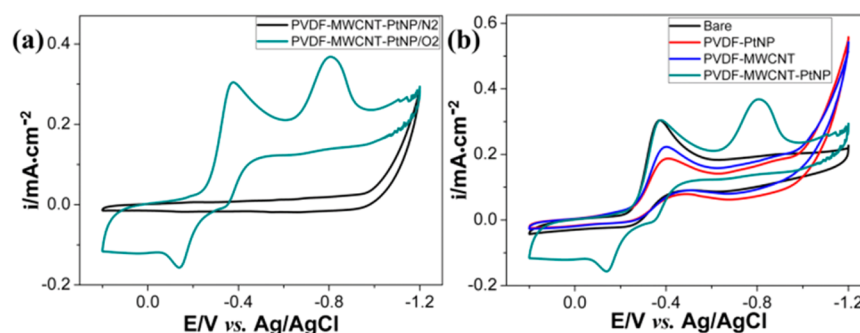
Figure 7. Catalysis of ORR: (a) PVDF−MWCNT−PtNP hybrid nanofibers/GCE in 0.1 M N$_2$-saturated and O$_2$-saturated KOH solution, respectively; (b) the same of a bare GCE, PVDF−PtNP/GCE, PVDF−MWCNT/GCE, and PVDF−MWCNT−PtNP hybrid nanofibers/GCE in 0.1 M O$_2$-saturated KOH solution at a scan rate of 50 mV/s.

should be attributed to the successful redox processes by the catalysis of the hybrid nanofibrous membrane. In addition, $I−T$ measurement with the applied potential of −0.41 V was carried out, and the rapid current response ranged from 15 to 100 mM (Figure 6b). It should be noted that, compared to H$_2$O$_2$ detection, the sensing performance of this biosensor for glucose is not very good, and it may be ascribed to two possible reasons. The first reason is that the hybrid nanofibrous membrane was attached not so strongly to the GCE in the test solution, and the other one is that the matrix polymer prevents the transport of electrons. In spite of this, the one-step electrospun nonenzymatic glucose sensor without calcination has several distinct advantages such as easy fabrication, high stability, time saving, and good reproducibility. The optimal experimental designs for better glucose biosensor performance are ongoing in our group.

ORR Catalysis Application. As the most active catalyst toward ORR, Pt-based metals have been widely studied recently. On the basis of the above characterizations, we know that MWCNTs are examined to act as wires for good electron transfer. In addition, PVDF can serve not only as the matrix but also as a binder in lithium-ion batteries.[56,57] Combining these three materials with private unique properties, the easy-prepared, stable, and high-efficiency ORR biocatalyst can be fabricated by electrospinning with high expectations.

Figure 7a shows the CVs of the fabricated PVDF−MWCNT−PtNP nanofibrous membrane modified GCE in N$_2$- and O$_2$-saturated 0.1 M KOH solution, respectively. Two well-defined peaks are present at −0.37 and −0.81 V in the O$_2$-saturated solution, while only a low capacitive current is presented in the N$_2$-saturated solution. To detect the catalysis property of the hybrid nanofiber membrane, the CVs of a bare GCE and PVDF−PtNP−, PVDF−MWCNT−, and PVDF−MWCNT−PtNP hybrid nanofibrous membrane modified GCEs in O$_2$-saturated 0.1 M KOH solution are presented in Figure 7b. For the bare GCE and PVDF−PtNP− and PVDF−MWCNT−modified GCEs, the electrochemical reduction starts at −0.45, −0.26, and −0.38 V, respectively. However, the PVDF−MWCNT−PtNP hybrid nanofibrous membrane modified GCE exhibits more positive onset potential (−0.14 V) and much larger reduction current for the ORR. This result greatly demonstrates the superior electrochemical ORR activity of the created PVDF−MWCNT−PtNP hybrid nanofibrous membrane. We suggest that the improved ORR activity is related to the special nanostructure of the created hybrid nanofibrous membrane. The nanoporous structure may maintain very high specific surface area, and the basic building blocks (PtNPs and MWCNTs) can provide enough active reaction sites, which activate the adsorption of O$_2$ on the surface of the hybrid nanofibrous membrane and promote the ORR process efficiently.[58,59]

CONCLUSIONS

In summary, we demonstrated a facile and efficient electrospinning technique to fabricate a novel piezoelectric β-phase PVDF−MWCNT−PtNP nanofibrous membrane on GCE and further investigated the potential applications as H$_2$O$_2$ and glucose biosensors, as well as for ORR catalysis. Compared to the previous reports, our strategy for producing hybrid nanofibrous membranes has several advantages, such as environmentally friendly, time saving, and highly efficient. Electrochemical data indicate that the PVDF−MWCNT−PtNP nanofibrous membrane performs good electrosensing activity toward H$_2$O$_2$ and glucose. The prepared biosensor based on this hybrid nanofibrous membrane shows a wide linear range, low detection limitation, high selectivity, and long-term stability. Moreover, excellent electrocatalysis as ORR catalyst was displayed. Several factors, such as the uniform dispersion of PtNPs, the axial orientation of CNTs, and the improved β-phase of PVDF, are the main reasons for promoting the electrochemical and eletrocatalysis properties of the electrospun PVDF−MWCNT−PtNP nanofibrous membrane. We believe that this electrospinning technique can be utilized to prepare other multifunctional nanomaterials, and the fabricated piezoelectric PVDF−MWCNT−PtNP nanofibrous membrane will have wide applications in actuator, generator, water purification, and energy storage.

AUTHOR INFORMATION

Corresponding Authors
*E-mail: wei@uni-bremen.de (G. Wei).
*E-mail: suzq@mail.buct.edu.cn (Z.Q. Su).

Notes
The authors declare no competing financial interest.

ACKNOWLEDGMENTS

■ REFERENCES

(1) Ronkainen, N. J.; Halsall, H. B.; Heineman, W. R. Electrochemical Biosensors. *Chem. Soc. Rev.* 2010, 39, 1747−1763.

(2) Wilson, G. S.; Hu, Y. Enzyme-Based Biosensors for in Vivo Measurements. *Chem. Rev.* 2000, 100, 2693−2704.

(3) Tseng, H.-W.; Tsai, Y.-J.; Yen, J.-H.; Chen, P.-H.; Yeh, Y.-C. A Fluorescence-Based Microbial Sensor for the Selective Detection of Gold. *Chem. Commun.* 2014, 50, 1735−1737.

(4) Munge, B. S.; Coffey, A.; Doucette, L. J. M.; Somba, B. K.; Malhotra, R.; Patel, V.; Gutkind, J. S.; Rusling, J. F. Nanostructured Immunosensor for Attomolar Detection of Cancer Biomarker Interleukin-8 Using Massively Labeled Superparamagnetic Particles. *Angew. Chem.* 2011, 123, 8061−8064.

(5) Shi, W.; Li, X.; Ma, H. A Tunable Ratiometric pH Sensor Based on Carbon Nanodots for the Quantitative Measurement of the Intracellular pH of Whole Cells. *Angew. Chem.* 2012, 124, 6538−6541.

(6) Sun, L.; Wu, J.; Du, F.; Chen, X.; Chen, Z. J. Cyclic GMP-AMP Synthase is a Cytosolic DNA Sensor that Activates the Type I Interferon Pathway. *Science* 2013, 339, 786−791.

(7) Heller, A.; Feldman, B. Electrochemistry in Diabetes Management. *Acc. Chem. Res.* 2010, 43, 963−973.

(8) Willner, I.; Willner, B. Biomolecule-Based Nanomaterials and Nanostructures. *Nano Lett.* 2010, 10, 3805−3815.

(9) Xiao, F.; Song, J.; Gao, H.; Zan, X.; Xu, R.; Duan, H. Coating Graphene Paper with 2D-Assembly of Electrocatalytic Nanoparticles: A Modular Approach toward High-Performance Flexible Electrodes. *ACS Nano* 2012, 6, 100−110.

(10) Chen, Y.-F.; Jiang, L.; Mancuso, M.; Jain, A.; Oncescu, V.; Erickson, D. Optofluidic Opportunities in Global Health, Food, Water and Energy. *Nanoscale* 2012, 4, 4839−4857.

(11) Zhai, D.; Liu, B.; Shi, Y.; Pan, L.; Wang, Y.; Li, W.; Zhang, R.; Yu, G. Highly Sensitive Glucose Sensor Based on Pt Nanoparticle/Polyaniline Hydrogel Heterostructures. *ACS Nano* 2013, 7, 3540−3546.

(12) Wang, Z.-G.; Wang, Y.; Xu, H.; Li, G.; Xu, Z.-K. Carbon Nanotube-Filled Nanofibrous Membranes Electrospun from Poly-(acrylonitrile-co-acrylic acid) for Glucose Biosensor. *J. Phys. Chem. C* 2009, 113, 2955−2960.

(13) Zhao, J.; Davidson, M. G.; Mahon, M. F.; Kociok-Kohn, G.; James, T. D. An Enantioselective Fluorescent Sensor for Sugar Acids. *J. Am. Chem. Soc.* 2004, 126, 16179−16186.

(14) Baratella, D.; Magro, M.; Sinigaglia, G.; Zboril, R.; Salviulo, G.; Vianello, F. A Glucose Biosensor Based on Surface Active Maghemite Nanoparticles. *Biosens. Bioelectron.* 2013, 45, 13−18.

(15) Li, J.; Li, Y.; Zhang, Y.; Wei, G. Highly Sensitive Molecularly Imprinted Electrochemical Sensor Based on the Double Amplification by an Inorganic Prussian Blue Catalytic Polymer and the Enzymatic Effect of Glucose Oxidase. *Anal. Chem.* 2012, 84, 1888−1893.

(16) Kimmel, D. W.; LeBlanc, G.; Meschievitz, M. E.; Cliffel, D. E. Electrochemical Sensors and Biosensors. *Anal. Chem.* 2012, 84, 685−707.

(17) Wang, J. Electrochemical Glucose Biosensors. *Chem. Rev.* 2008, 108, 814−825.

(18) Heller, A.; Feldman, B. Electrochemical Glucose Sensors and Their Applications in Diabetes Management. *Chem. Rev.* 2008, 108, 2482−2505.

(19) Lang, X.-Y.; Fu, H.-Y.; Hou, C.; Han, G.-F.; Yang, P.; Liu, Y.-B.; Jiang, Q. Nanoporous Gold Supported Cobalt Oxide Microelectrodes as High-Performance Electrochemical Biosensors. *Nat. Commun.* 2013, 4, 2169.

(20) Nichols, S. P.; Koh, A.; Storm, W. L.; Shin, J. H.; Schoenfisch, M. H. Biocompatible Materials for Continuous Glucose Monitoring Devices. *Chem. Rev.* 2013, 113, 2528−2549.

(21) Zhang, P.; Zhang, X.; Zhang, S.; Lu, X.; Li, Q.; Su, Z.; Wei, G. One-Pot Green Synthesis, Characterizations, and Biosensor Application of Self-Assembled Reduced Graphene Oxide-Gold Nanoparticle Hybrid Membranes. *J. Mater. Chem. B* 2013, 1, 6525−6531.

(22) Lu, J.; Do, I.; Drzal, L. T.; Worden, R. M.; Lee, I. Nanometal-Decorated Exfoliated Graphite Nanoplatelet Based Glucose Biosensors

with High Sensitivity and Fast Response. *ACS Nano* 2008, 2, 1825−1832.

(23) Karam, P.; Halaoui, L. I. Sensing of H_2O_2 at Low Surface Density Assemblies of Pt Nanoparticles in Polyelectrolyte. *Anal. Chem.* 2008, 80, 5441−5448.

(24) Bai, H.; Han, M.; Du, Y.; Bao, J.; Dai, Z. Facile Synthesis of Porous Tubular Palladium Nanostructures and Their Application in A Nonenzymatic Glucose Sensor. *Chem. Commun.* 2010, 46, 1739−1741.

(25) Wang, G.; Lu, X.; Zhai, T.; Ling, Y.; Wang, H.; Tong, Y.; Li, Y. Free-Standing Nickel Oxide Nanoflake Arrays: Synthesis and Application for Highly Sensitive Non-Enzymatic Glucose Sensors. *Nanoscale* 2012, 4, 3123−3127.

(26) Lee, H.; Yoon, S. W.; Kim, E. J.; Park, J. In-Situ Growth of Copper Sulfide Nanocrystals on Multiwalled Carbon Nanotubes and Their Application as Novel Solar Cell and Amperometric Glucose Sensor Materials. *Nano Lett.* 2007, 7, 778−784.

(27) Wu, J.; Yang, H. Platinum-Based Oxygen Reduction Electrocatalysts. *Acc. Chem. Res.* 2013, 46, 1848−1857.

(28) Chen, A.; Holt-Hindle, P. Platinum-Based Nanostructured Materials: Synthesis, Properties, and Applications. *Chem. Rev.* 2010, 110, 3767−3804.

(29) Baughman, R. H.; Zakhidov, A. A.; de Heer, W. A. Carbon Nanotubes-the Route toward Applications. *Science* 2002, 297, 787−792.

(30) Musameh, M.; Notivoli, M. R.; Hickey, M.; Kyratzis, I. L.; Gao, Y.; Huynh, C.; Hawkins, S. C. Carbon Nanotube Webs: A Novel Material for Sensor Applications. *Adv. Mater.* 2011, 23, 906−910.

(31) Li, W.; Liang, C.; Qiu, J.; Zhou, W.; Han, H.; Wei, Z.; Sun, G.; Xin, Q. Carbon Nanotubes as Support for Cathode Catalyst of A Direct Methanol Fuel Cell. *Carbon* 2002, 40, 787−803.

(32) Hrapovic, S.; Liu, Y.; Male, K. B.; Luong, J. H. T. Electrochemical Biosensing Platforms Using Platinum Nanoparticles and Carbon Nanotubes. *Anal. Chem.* 2004, 76, 1083−1088.

(33) Yang, M.; Yang, Y.; Liu, Y.; Shen, G.; Yu, R. Platinum Nanoparticles-Doped Sol-Gel/Carbon Nanotubes Composite Electrochemical Sensors and Biosensors. *Biosens. Bioelectron.* 2006, 21, 1125−1131.

(34) Wu, B.; Hu, D.; Kuang, Y.; Liu, B.; Zhang, X.; Chen, J. Functionalization of Carbon Nanotubes by an Ionic-Liquid Polymer: Dispersion of Pt and PtRu Nanoparticles on Carbon Nanotubes and Their Electrocatalytic Oxidation of Methanol. *Angew. Chem., Int. Ed.* 2009, 48, 4751−4754.

(35) Zhao, Y.; Fan, L.; Zhong, H.; Li, Y.; Yang, S. Platinum Nanoparticle Clusters Immobilized on Multiwalled Carbon Nanotubes: Electrodeposition and Enhanced Electrocatalytic Activity for Methanol Oxidation. *Adv. Funct. Mater.* 2007, 17, 1537−1541.

(36) Wildgoose, G. G.; Banks, C. E.; Compton, R. G. Metal Nanoparticles and Related Materials Supported on Carbon Nanotubes: Methods and Applications. *Small* 2006, 2, 182−193.

(37) Luo, C. J.; Stoyanov, S. D.; Stride, E.; Pelan, E.; Edirisinghe, M. Electrospinning versus Fibre Production Methods: From Specifics to Technological Convergence. *Chem. Soc. Rev.* 2012, 41, 4708−4735.

(38) Miao, J.; Miyauchi, M.; Simmons, T. J.; Dordick, J. S.; Linhardt, R. J. Electrospinning of Nanomaterials and Applications in Electronic Components and Devices. *J. Nanosci. Nanotechnol.* 2010, 10, 5507−5519.

(39) Su, Z.; Li, J.; Ouyang, Z.; Arras, M. M. L.; Wei, G.; Jandt, K. D. Biomimetic 3D Hydroxyapatite Architectures with Interconnected Pores Based on Electrospun Biaxially Orientated PCL Nanofibers. *RSC Adv.* 2014, 4, 14833−14839.

(40) Wang, J.; Yao, H. B.; He, D.; Zhang, C. L.; Yu, S. H. Facile Fabrication of Gold Nanoparticles-Poly(vinyl alcohol) Electrospun Water-Stable Nanofibrous Mats: Efficient Substrate Materials for Biosensors. *ACS Appl. Mater. Interfaces* 2012, 4, 1963−1971.

(41) Ouyang, Z.; Li, J.; Wang, J.; Li, Q.; Ni, T.; Zhang, X.; Wang, H.; Li, Q.; Su, Z.; Wei, G. Fabrication, Characterization and Sensor Application of Electrospun Polyurethane Nanofibers Filled with

Carbon Nanotubes and Silver Nanoparticles. *J. Mater. Chem. B* **2013**, *1*, 2415−2424.

(42) Cha, S. N.; Kim, S. M.; Kim, H. J.; Ku, J. Y.; Sohn, J. I.; Park, Y. J.; Song, B. G.; Jung, M. H.; Lee, E. K.; Choi, B. L.; Park, J. J.; Wang, Z. L.; Kim, J. M.; Kim, K. Porous PVDF as Effective Sonic Wave Driven Nanogenerators. *Nano Lett.* **2011**, *11*, 5142−5147.

(43) Naber, R. C. G.; Asadi, K.; Blom, P. W. M.; de Leeuw, D. M.; de Boer, B. Organic Nonvolatile Memory Devices Based on Ferroelectricity. *Adv. Mater.* **2010**, *22*, 933−945.

(44) Bae, J.; Song, M. K.; Park, Y. J.; Kim, J. M.; Liu, M.; Wang, Z. L. Fiber Supercapacitors Made of Nanowire-Fiber Hybrid Structures for Wearable/Flexible Energy Storage. *Angew. Chem., Int. Ed.* **2011**, *50*, 1−6.

(45) Hattori, T.; Hikosaka, M.; Ohigashi, H. The Crystallization Behaviour and Phase Diagram of Extended-Chain Crystals of Poly(vinylidene fluoride) under High Pressure. *Polymer* **1996**, *37*, 85−91.

(46) Singh, R.; Kumar, J.; Singh, R. K.; Kaur, A.; Sinha, R. D. P.; Gupta, N. P. Low Frequency ac Conduction and Dielectric Relaxation Behavior of Solution Grown and Uniaxially Stretched Poly(vinylidene fluoride) Films. *Polymer* **2006**, *47*, 5919−5928.

(47) Baji, A.; Mai, Y.-W.; Li, Q.; Liu, Y. Electrospinning Induced Ferroelectricity in Poly(vinylidene fluoride) Fibers. *Nanoscale* **2011**, *3*, 3068−3071.

(48) Andrew, J. S.; Clarke, D. R. Effect of Electrospinning on the Ferroelectric Phase Content of Polyvinylidene Difluoride Fibers. *Langmuir* **2008**, *24*, 670−672.

(49) Dror, Y.; Salalha, W.; Khalfin, R. L.; Cohen, Y.; Yarin, A. L.; Zussman, E. Carbon Nanotubes Embedded in Oriented Polymer Nanofibers by Electrospinning. *Langmuir* **2003**, *19*, 7012−7020.

(50) Salalha, W.; Dror, Y.; Khalfin, R. L.; Cohen, Y.; Yarin, A. L.; Zussman, E. Single-Walled Carbon Nanotubes Embedded in Oriented Polymeric Nanofibers by Electrospinning. *Langmuir* **2004**, *20*, 9852−9855.

(51) Lovinger, A. J. Ferroelectric Polymers. *Science* **1983**, *220*, 1115−1121.

(52) Zhong, G.; Zhang, L.; Su, R.; Wang, K.; Fong, H.; Zhu, L. Understanding Polymorphism Formation in Electrospun Fibers of Immiscible Poly(vinylidene fluoride) Blends. *Polymer* **2011**, *52*, 2228−2237.

(53) Zheng, J.; He, A.; Li, J.; Han, C. C. Polymorphism Control of Poly(vinylidene fluoride) through Electrospinning. *Macromol. Rapid Commun.* **2007**, *28*, 2159−2162.

(54) Su, Z.; Li, J.; Li, Q.; Ni, T.; Wei, G. Chain Conformation, Crystallization Behavior, Electrical and Mechanical Properties of Electrospun Polymer-Carbon Nanotube Hybrid Nanofibers with Different Orientations. *Carbon* **2012**, *50*, 5605−5617.

(55) Wei, G.; Xu, F.; Li, Z.; Jandt, K. D. Protein-Promoted Synthesis of Pt Nanoparticles on Carbon Nanotubes for Electrocatalytic Nanohybrids with Enhanced Glucose Sensing. *J. Phys. Chem. C* **2011**, *115*, 11453−11460.

(56) Lee, J. K.; Smith, K. B.; Hayner, C. M.; Kung, H. H. Silicon Nanoparticles-Graphene Paper Composites for Li Ion Battery Anodes. *Chem. Commun.* **2010**, *46*, 2025−2027.

(57) Wang, D.; Choi, D.; Li, J.; Yang, Z.; Nie, Z.; Kou, R.; Hu, D.; Wang, C.; Saraf, L. V.; Zhang, J.; Aksay, I. A.; Liu, J. Self-Assembled TiO_2-Graphene Hybrid Nanostructures for Enhanced Li-Ion Insertion. *ACS Nano* **2009**, *3*, 907−914.

(58) Wang, F.-B.; Wang, J.; Shao, L.; Zhao, Y.; Xia, X.-H. Hybrids of Gold Nanoparticles Highly Dispersed on Graphene for the Oxygen Reduction Reaction. *Electrochem. Commun.* **2014**, *38*, 82−85.

(59) Xu, S.; Yong, L.; Wu, P. One-Pot, Green, Rapid Synthesis of Flowerlike Gold Nanoparticles/Reduced Graphene Oxide Composite with Regenerated Silk Fibroin As Efficient Oxygen Reduction Electrocatalysts. *ACS Appl. Mater. Interfaces* **2013**, *5*, 654−662.